DOI: 10.1002/ ((please add manuscript number))
Article type: Full Paper

Polymorph Selectivity of Coccolith-Associated Polysaccharides from *Gephyrocapsa oceanica* on Calcium Carbonate Formation *In Vitro*

Author(s), and Corresponding Author(s): Jessica M. Walker, Bartosz Marzec, Renee B. Y. Lee, Kristyna Vodrazkova, Sarah J. Day, Chiu C. Tang, Rosalind E. M. Rickaby, Fabio Nudelman**

Dr. J. M. Walker, Dr. B. Marzec, K. Vodrazkova, Dr. F. Nudelman
School of Chemistry, University of Edinburgh, Joseph Black Building, David Brewster Road, Edinburgh, EH9 3FJ
E-mail: Fabio.nudelman@ed.ac.uk

Dr. R. B. Y. Lee
School of Biological Sciences, University of Reading, Hopkins Building, Whiteknights, Reading, Berkshire, RG6 6UB

Dr. S. J. Day, Prof. C. C. Tang
Diamond Light Source, Harwell Science and Innovation Campus, Didcot, Oxfordshire, OX11 0DE, UK

Prof. R. E. M. Rickaby
Department of Earth Sciences, University of Oxford, South Parks Road, Oxford, OX1 3AN

Keywords: coccolithophores, biomineralization, calcite, cryo-transmission electron microscopy, crystal nucleation

Coccolith-associated polysaccharides (CAPs) are thought to be a key part of the biomineralization process in coccolithophores, however their role is not fully understood. We have used two different systems that promote different polymorphs of calcium carbonate to show the effect of CAPs on nucleation and polymorph selection *in vitro*. Using a combination of time-resolved cryo-transmission electron microscopy (cryoTEM) and scanning electron microscopy (SEM), we examined the mechanisms of calcite nucleation and growth in the presence of the intracrystalline fraction containing CAPs extracted from coccoliths from *Gephyrocapsa oceanica* and *Emiliania huxleyi*, two closely related coccolithophore species. The CAPs extracted from *G. oceanica* were shown to promote calcite nucleation *in vitro*,

even under conditions favouring the kinetic products of calcium carbonate, vaterite and aragonite. This was not the case with CAPs extracted from *E. huxleyi*, suggesting that the functional role of CAPs *in vivo* may be different between the two species. Additionally, high-resolution synchrotron powder X-ray diffraction (SXPD) revealed that the polysaccharide is located between grain boundaries of both calcite produced in the presence of the CAPs *in vitro* and biogenic calcite, rather than within the crystal lattice.

1. Introduction

Biomineralization is the production of mineralized tissues by organisms, and is widespread throughout the five kingdoms. From teeth for grinding to bones and shells for structure, organisms have long exploited crystal properties to suit their functional requirements.[1] Coccolith scales, produced by coccolithophores, which are unicellular calcifying marine algae, are a striking example of the fine control that organisms exert over mineral formation.[2] Each coccolith scale is an assembly of nano-crystalline building blocks of $CaCO_3$ in the form of calcite that are mechanically interlocked into an elliptical structure (**Figure 1**).[3] The crystals exhibit non-equilibrium morphologies and have precisely controlled crystallographic orientations. Furthermore, the morphology of the calcite crystals produced by coccolithophores is species-specific, to the extent that their taxonomic classification is based on the size and shape of the coccoliths.[4] In contrast, non-biogenic calcite crystals are at least a few micrometres in size and have a rhombohedral morphology, reflective of the unit cell. Due to the precise level of control coccolithophores exert over the nucleation, growth and morphology of the calcite crystals, many studies have explored the mechanism by which this is achieved (e.g [5]).

Each coccolith is formed inside a specialized intracellular compartment that is derived from the Golgi complex called the coccolith vesicle.[6] Mineral formation starts with the

nucleation of calcite crystals on the rim of an organic scaffold known as a baseplate, forming a proto-coccolith ring, followed by crystal growth.[3] Once mature, the vesicle is secreted towards the cell surface, and the coccolith is extruded to the exterior of the cell. At least two sets of macromolecules are present in the vesicle during coccolithogenesis: the aforementioned organic scaffold, or baseplate, which is water-insoluble,[3, 7] and the water-soluble coccolith-associated polysaccharides (CAPs), which are the predominant organic components associated with calcification in coccolithophores.[8]

Little is known about the roles of these macromolecules in controlling the biomineralization process and how conserved their function may be across species and morphotypes. However, it is thought that the baseplates, composed of cellulose fibres and proteins,[9] use a structured template to serve as a scaffold for crystal nucleation and growth,[3, 10] whilst the CAPs are purported to be involved in regulating the transport of Ca^{2+} ions, promoting crystal growth and determining morphology.[5a] Recently, Gal *et* al. demonstrated that polysaccharides from *Pleurochrysis carterae* selectively bind to the rim of the baseplates in the presence of calcium ions, suggesting that both components act cooperatively to direct the ions to the mineralization site.[9]

The CAPs are acidic in nature, with those originating from *Emiliania huxleyi* known to consist of a backbone of mannose residues with attached complex side-chains that contain both sulfate esters and uronic acid groups, the latter mostly consisting of galacturonic acid.[11] The structure and composition of CAPs differ between species, with some species such as *P. carterae* requiring more than one CAP during mineralization.[8a, 12] Such variance is particularly evident in the uronic acid content of the CAPs which varies between both strains and species and was suggested to have an impact on the final morphology of the resulting coccoliths.[11a]

In vitro studies have shown that CAPs isolated from *E. huxleyi* inhibits calcite growth by adsorbing to the acute $[\bar{4}41]$- and $[48\bar{1}]$-edges of calcite and generating crystals elongated along the *c*-axis.[5a, 10] Moreover, adsorption to the calcite acute steps only occurred in the pH range of 3.4 to 7.7 and in the presence of K^+, Na^+, Sr^{2+} and Ca^{2+} ions, suggesting that polysaccharide conformation and reaction conditions are important for function.[13] Indeed, while the carboxylic acid moiety of uronic groups of CAPs is proposed to be responsible for its activity in affecting calcite growth due to its ability to bind Ca^{2+} ions, polygalacturonic acid at a similar concentration does not show the same effect.[11a, 14] However, investigations on calcite growth in the presence of CAPs have so far been limited to studying their effect on crystal morphology, or their interaction with an already formed calcite surface.[5a, 13] Therefore, whether CAPs induce crystal nucleation or have any polymorph selectivity properties remains unknown.

While most research has been conducted on CAPs extracted from the distantly related *E. huxleyi* and *P. carterae*, little is known about the polysaccharides from other coccolithophore species and how they affect calcite formation. Here, we investigated the effect of an intracrystalline fraction composed of polysaccharides extracted from *Gephyrocapsa oceanica*, considered a 'sister species' to *E. huxleyi*, on $CaCO_3$ precipitation *in vitro* to understand how this macromolecule affects and controls crystal nucleation and growth. *G. oceanica* is closely related to *E. huxleyi*, having diverged only 291,000 years ago,[15] however, distinct differences exist between the species: *G. oceanica* has a larger cell size, and more heavily calcified coccoliths which display a central bridge formation. Examples of coccoliths from both *G. oceanica* and *E. huxleyi* are shown in Figure 1. These two species contain only one type of CAP, which are found inside the calcite crystals during coccolith formation, and can be purified by dissolving the mineral.[11a, 16] Lee et al. described differences in the polysaccharides between these two species, showing *G. oceanica* CAPs to

be smaller but little data are available regarding the nature and action of *G. oceanica* CAPs on calcite nucleation and growth.[11a] Using a combination of scanning electron microscopy (SEM), cryo-transmission electron microscopy (cryoTEM), powder X-ray diffraction (pXRD) and high-resolution synchrotron X-ray powder diffraction (SXPD) we demonstrate that the intracrystalline fraction from *G. oceanica* has a unique property of calcite selectivity, even under conditions that would normally favour other $CaCO_3$ polymorphs. We suggest that this polymorph selectivity plays a biological role in coccolithogenesis in *G. oceanica*.

2. Results

2.1. Crystallization in the Presence of CAPs

The intracrystalline organic fraction of the coccoliths from *E. huxleyi* and *G. oceanica*, composed mainly of CAPs, was extracted by dissolving the crystals and isolated as previously described.[11a] SDS-PAGE confirmed that the intracrystalline fractions from each species was composed of polysaccharides of a single molecular weight, visible by the presence of a single band on the Alcian Blue-stained gel (Supporting Information, **Figure S1**). Furthermore, no proteins were detected by coomassie-stained gel (Supporting Information, **Figure S2**) or by Bradford assay, showing the absence of these macromolecules from the extracts.

To examine the effect of the CAPs on calcium carbonate nucleation and polymorph selectivity, we utilized a direct addition method where Na_2CO_3 was added directly to $CaCl_2.2H_2O$ to create a final reaction concentration of 5 mM of each, with or without the presence of each polysaccharide individually at a concentration of 5 µg/mL. Using these high supersaturation conditions favours the formation of the kinetic products of $CaCO_3$ expected at this temperature - vaterite and amorphous calcium carbonate (‘ACC’) - in addition to calcite. Furthermore, this system has a pH of *ca.* 10.8, in which no calcite step adsorption of the CAP

is observed,[13] precluding any morphological effect on $CaCO_3$ formation. Thus, these conditions allow us to investigate exclusively the effect of the CAPs on crystal nucleation and polymorph type. The polysaccharides employed in this study were extracted from *E. huxleyi*, (strain RCC1216) and from *G. oceanica* (strain RCC1314). Both CAPs have consistent uronic acid contents of 58.5 % and 54.75 % which is significant given that these moieties are thought to be responsible for Ca^{2+} binding.[11a]

To observe the crystals formed in the reaction, glass slides were removed from the base of the reaction solution after 20 minutes of reaction and examined by SEM and Raman spectroscopy. When no additives were present, two contrasting morphologies were observed; rhombohedral and spherical. These represent a mixture of calcite and vaterite respectively, with the identity of the polymorphs confirmed by Raman spectroscopy (Supporting Information, **Figure S3**). This mixture of polymorphs was also observed when *E. huxleyi* CAPs were added to the reaction solution. However, in the presence of *G. oceanica* CAPs, no vaterite was observed, and only calcite was present. Representative SEM images of the species found in each sample are shown in **Figure 2a-c**.

To examine this further, a minimum of 300 crystals per sample from SEM images were measured for the control and each polysaccharide. The ratio of crystals of the two polymorphs in the control and in the presence of the *E. huxleyi* CAPs was shown to be 90% vaterite to 10% calcite, whilst it was confirmed that in the presence of *G. oceanica* CAPs, consistently only calcite was present (Figure 2a). Additionally, results showed a difference in both number of crystals per mm^2 and size (Figures 2b and c). While the control and the *E. huxleyi* polysaccharide yielded about 200-300 crystals per mm^2, in the presence of the CAPs from *G. oceanica* the number of crystals per mm^2 increased to 8300. This was concurrent with a decrease in the size of the crystals formed when the latter was present, going from 13-15 µm to 2.5-3 µm (Figure 2c). This demonstrates that the *G. oceanica* CAPs promoted

calcite nucleation. As nucleation events happen more frequently, more crystals form in the same amount of time, resulting in a faster drop in the supersaturation of the growth mixture. Therefore, the size of the crystals is smaller when compared with reference samples. Comparison of the two species, both in terms of polymorph mixture and nucleating ability, shows that even with similar uronic acid contents the two CAPs do not produce the same effect, which provides evidence that another aspect of these molecules must be taken into consideration while investigating their effect on calcium carbonate precipitation.

2.2. Time resolved Examination of the Reaction Solution

To further explore this interesting property, time-resolved SEM was used to examine the effect of *G. oceanica* CAPs on the reaction mechanism (**Figure 3**). When no additives were present, an initial precursor of spherical amorphous calcium carbonate (ACC, demonstrated by low dose selected area diffraction (LDSAED), **Figure 4a**, inset) particles of 250-350 nm formed after 1 minute (Figure 3a). These particles then began to aggregate (Figure 3b), with crystalline material first observed after 10 minutes (Figure 3c). After 20 minutes, a mixture of calcite and vaterite was present (Figure 3d). Contrastingly, in the presence of *G. oceanica* CAPs, the initial ACC formed after 1 minute was 50-150 nm, a marked decrease in size compared to the control system. The particles were irregular in shape and size, and semi-cuboid shapes were already beginning to form (red circle, Figure 3e). Calcite rhombohedra were visible by 3 minutes, surrounded by an attached flat material, with the continued presence of small ACC particles (Figure 3f). These were angular in texture, as shown in higher magnification in Figure 3g. By 10 minutes, fully formed calcite was present (Figure 3h), with only a small amount of ACC remaining. All ACC was gone by 15 minutes (Supporting Information, **Figure S4**). The fast precipitation and growth of calcite in the presence of the *G. oceanica* CAPs suggest it is acting as a nucleator for the polymorph, and

the decrease in size observed in the ACC is likely due to the co-precipitation of small calcite crystals which provide a sink for calcium and carbonate ions. These observations support the conclusions drawn from the results in Figure 2.

In order to obtain a mechanistic understanding of the crystallization process induced by *G. oceanica* CAPs, time-resolved cryo-transmission electron microscopy (cryoTEM) was employed to visualize particles present in the reaction solution at early time points in their native, hydrated state. For this, samples were collected at different time points throughout the reaction, plunge-frozen in liquid ethane and analyzed by cryoTEM. Similar to the results obtained with the SEM, without additives, after 1 minute spherical particles of 250-350 nm were present in the reaction (Figure 4a, red circle). Low dose selected area diffraction (LDSAED) did not show any signs of crystallinity, confirming that they were composed of ACC (Figure 4a, inset). After 10 minutes the amount of ACC had increased, and the particles started to aggregate (Figure 4b), and after 20 minutes crystallized into a mixture of vaterite (Figure 4c, red arrow) and calcite (Figure 4c, white arrow), as demonstrated by LDSAED (Figure 4c, inset).

When *G. oceanica* CAPs were present, after 1 minute irregular particles of ACC 45-100 nm were visible (Figure 4d), shown to be amorphous by LDSAED (Figure 4d, inset). By 3 minutes, (Figure 4e) the material had begun to crystallize, with the first crystals of calcite, around 100 nm in size, present (Figure 4e, inset). After 40 minutes, only calcite crystals were present (Figure 4f). Here, several smaller crystals were found to be connected to a larger central one, analogous to the crystals shown by SEM (Figure 3f), suggesting Ostwald ripening is taking place to continue the crystal growth.

From these results we can see a number of changes taking place in the presence of *G. oceanica* CAPs. The polysaccharide has had a major effect on the mechanism of calcite formation in terms of both nucleation and growth of calcite. Initial ACC formed is smaller

and has a different and irregular morphology. Calcite growth is observed at an earlier time point, with more nucleation points, resulting in many small crystals, and suggesting that rather than disfavouring vaterite, calcite is being actively selected.

2.3 Effect of Polysaccharides in an Aragonite Promoting System

To directly address whether indeed the CAPs disfavour the formation of vaterite specifically, or produces a nucleating effect that can favour calcite in systems where it is not the preferential polymorph, we investigated the effect of the CAPs (at the same concentration of 5 µg/mL) in a secondary system. The chosen system used a 1:1 water:alcohol mixture to specifically promote the formation of aragonite by dramatically increasing the supersaturation of carbonate within the water phase of the solution.[17] Dynamic light scattering and cryoTEM measurements confirmed that the CAPs from *E. huxleyi* and *G. oceanica* remained soluble in 50 % ethanol (Supporting Information, **Figure S5**). Glass slides from each reaction were removed after 24 hours and examined under SEM to observe any changes. Refined powder X-ray diffraction patterns were used to quantify the ratio of aragonite to calcite. As expected, in the control experiments where CAPs were absent, >95 % of aragonite was obtained (**Figure 5**a and e). Again, we saw little effect from the *E. huxleyi* CAPs (Figure 5b) when compared to the control (Figure 5a), but a marked increase in calcite in the presence of *G. oceanica* CAPs (Figure 5c), from 5 % to 40 %. This provides evidence that a biological material can direct polymorph selectivity even in this synthetic system, where the driving force is highly favoured towards aragonite.

Lowering the concentration to 1 µg/mL resulted in a decrease in the amount of calcite (Supporting Information, **Figure S6**), showing a correlation between concentration of polysaccharide and amount of calcite present in the sample. Experiments using higher concentrations of the polysaccharide were not possible due to the limited availability of the

material. To further confirm that the uronic acid alone is not responsible for promoting calcite, we used polygalacturonic acid (≥85%, Sigma Aldrich) as an additive in the experiment. Similar to the control and the CAPs from *E. huxleyi,* the amount of calcite formed still remained at under 10 % (Figure 5d).

Time resolved cryoTEM of this aragonite promoting system in the presence of *G. oceanica* CAPs also showed the fast formation of calcite crystals (**Figure 6**). In control experiments, where no additives were present, precipitation started with the formation of ACC particles (60-120 nm) after 3 minutes (Figure 6a and LDSAED, inset), which grew in size and aggregated after 10 minutes (Figure 6b and LDSAED, inset), leading to the formation of aragonite crystals after 1 hour (Figures 6c and 6g).[18] In contrast, in the presence of the CAPs from *G. oceanica,* calcite crystals several hundreds of nanometres in size were already present after 1 minute (Figure 6d), and were continuously forming in the solution as evidenced by the presence of calcite crystals of similar size after 5 minutes and 40 minutes (Figure. 6d-k). As ACC was also present at 1 minute (Supporting Information, **Figure S7**), this suggests that two competing pathways are present in the system. One, via ACC, leads to aragonite as the favoured polymorph, and the second is the direct nucleation of calcite by *G. oceanica* CAPs. This is supported by the observations that the size of the ACC particles formed in this system when the CAPs was present were smaller than in the control: 30-160 nm in the former (Supporting Information, Figure S6a), as opposed to 60-120 nm in the latter (Figure 6a). Additionally, after 5 minutes some larger ACC particles were occasionally present (Figure 6e and Supporting Information Figure S6b), but were much less prevalent than in the absence of additives (Figure 6b). This is reflective of observations for the direct addition system. Interestingly, no aragonite crystals were found in the cryoTEM analysis of the samples precipitated in the presence of *G. oceanica* CAPs. As we know from the SEM experiments that this polymorph does still form (Figure 5), this further supports the

conclusion that two different pathways are present at the same time: one leading to calcite, nucleated by the CAPs, and one leading to aragonite due to the water:alcohol mixture. This allows us to confirm that the CAPs are actively selecting calcite rather than disfavouring the other polymorphs of calcium carbonate.

Additional control experiments were performed using CAPs extracted following the methods by de Jong et al.,[19] and Gal et al.[9], none of which involve treating the coccoliths with NaOCl prior to polysaccharide extraction. As before, CAPs from *E. huxleyi* did not promote calcite formation when precipitation was carried out using a reaction mixture containing 5 mM of $CaCl_2$ and 5 mM of Na_2CO_3 (Supporting information, **Figure S8a and b**). Rather, a similar proportion of vaterite as the control was obtained. Similarly, the CAPs had little effect in promoting calcite formation under aragonite-promoting conditions (Supporting information, **Figure S8c and d**). CAPs from *G. oceanica*, on the other hand, promoted calcite formation under both experimental conditions (Supporting information, **Figure S9**). This demonstrates that that the lack of polymorph selectivity activity by the *E. huxleyi* is not due to oxidative damaged caused by the NaOCl, but rather due to the composition and structure of the macromolecules.

2.4 Synchrotron Powder X-Ray Diffraction

To examine whether the polysaccharide occludes within the crystal lattice, synchrotron SXPD was used to examine the lattice distortion and coherence length (the single crystalline domain size) in calcite crystals grown in the presence of *G. oceanica* CAPs. Previous work has shown that incorporation of amino acids into the calcite lattice causes a significant shift in the lattice distortion.[20] The two most pronounced examples were aspartic acid and cysteine whose incorporation led to lattice deviation of $\Delta a/a=2.33 \times 10^{-3}$ and $\Delta c/c=1.56 \times 10^{-3}$ respectively. Here we consider a polysaccharide, so it would be expected

that any incorporation would produce a shift at least equal to individual amino acids (therefore on the scale of 10^{-3}). Rietveld refinement of the resulting patterns showed the lattice distortion ($\Delta c/c$) for the (*104*)-plane to be on the scale of 10^{-4} for crystals grown in the presence of *G. oceanica* CAPs, demonstrating that there was limited incorporation into the lattice **(Figure 7b)**. Similar results were obtained in the analysis of the biogenic coccoliths from *G. oceanica*, which exhibited a lattice distortion of 3.6 x 10^{-4} (Figure 7c), well below the expected shift (refined fitted curves for (*104*)-reflection and full patterns are shown in **Figure S10 and S11**, Supporting Information). In contrast, peak broadening was significant in both samples. Since the SXPD instrumental contributions are negligible due to its high resolution capability,[21] this must be attributed either to a decrease in the coherence length or lattice strain.

The dominantly Lorentzian broadening of the reflections described by a pseudo-Voigt function confirmed that coherence length of the crystal domains provided the major contribution to broadening. Interestingly, both calcite grown in the presence of *G. oceanica* CAP and coccolith calcite produced by *G. oceanica* cells have a similar level of broadening (Figure 7b and c) and similar coherence lengths of 373 nm and 343 nm respectively, calculated using the Scherrer equation. In contrast, a control sample (Figure 7a) precipitated under the same conditions produced crystals characterized with a coherence length of 800 nm. Taken together, the SXPD data shows that *G. oceanica* polysaccharide, produced both *in vitro* and in biogenic calcite is located in the grain boundaries of the crystals, rather than in the crystal lattice. This is in agreement with earlier work on another species of coccolithophore, *P. carterae.*[16b] We attempted to quantify the amount of polysaccharides occluded within the calcite single crystals, however, this was technically challenging as the amount of material is below the detection limit of methods at our disposal.

3. Discussion

Our results show that, *in vitro*, there is a strong driving force for the formation of calcite when the intracrystalline CAPs from *G. oceanica* coccoliths are present, an ability not evident at the same concentration of *E. huxleyi* CAPs (Figure 1 and 3). Previous work on CAPs has focused on *E. huxleyi*, which can inhibit $CaCO_3$ precipitation.[5a, 14] This is clearly not the case for *G. oceanica*, where calcite nucleation is strongly favoured under our experimental conditions. The identification of a calcite preference over two different polymorphs suggests an active selectivity for calcite rather than a mechanism where both competing polymorphs are disfavoured. Although we are unable to confirm whether this *in vitro* effect is present *in vivo*, it raises interesting questions about the contrasting process of coccolithogenesis in *G. oceanica* compared to *E. huxleyi*.

The time-resolved studies show an increase in the rapidity of appearance of calcite crystals, which takes place after only 1 minute of reaction in the presence of *G. oceanica* CAPs in both systems (Figure 3 and 6). This is opposed to the control, where 20 minutes is required to observe fully formed crystals (Figure 3a-d). When considered alongside the increase in number of crystals in the presence of the CAPs, this early calcite growth indicates that the polysaccharide is acting as a calcite nucleator.

It has previously been shown that several mechanisms of calcite formation can occur concurrently in a system.[22] Our results suggest that in the two systems investigated here (direct addition and water:ethanol mixture), two competing mechanisms were taking place simultaneously when the CAPs were added: one progressing via ACC that will eventually crystallize into the favoured polymorph according to the solution conditions (i.e. vaterite and calcite in the direct addition method or aragonite in water:ethanol mixture), and the other mechanism progressing via direct nucleation of calcite induced by the CAPs. Since calcite is the most thermodynamically stable polymorph of $CaCO_3$, its presence in the reaction from

the very early stages induced dissolution-reprecipitation, where calcite grew at the expense of the ACC. As a result, no vaterite was observed in the direct addition method and 40 % calcite formed in the water:ethanol mixture. It is possible that in the latter case, a higher proportion of calcite could be obtained if a higher concentration of the CAPs is used.

The small lattice distortion and consequential lack of incorporation of the polysaccharide within the crystal lattice (Figure 7) shows the mechanism differs from other mechanisms of polymorph selectivity such as the promotion of aragonite in the presence of Mg^{2+} ions. In the cases of Mg^{2+}, the ions incorporate into the lattice in sufficient amounts to make calcite unfavourable, thereby promoting aragonite.[23] As we observe no significant lattice distortion in calcite crystals grown in the presence of the polysaccharide, we can discount this mechanism. This was expected considering that the polysaccharide is a large molecule, and therefore is more likely to be situated at the grain boundary, rather than inside the crystal lattice. This is in agreement with previous work on the occlusion of coccolithophore macromolecules.[16b] This is confirmed by the decrease in the coherence length observed in the presence of *G. oceanica* CAPs and coccoliths (Figure 7b and c), which means that within the crystals formed, sizes of individual domains are smaller compared to the reference sample. This is consistent with other biominerals, which show decreased coherence length in comparison to non-biogenic crystals due to the occlusion of macromolecules.[24] This provides evidence that the polysaccharide is active in solution and at the solution/crystal interface.

It has been shown that the *E. huxleyi* CAPs attach preferentially onto the acute edge of calcite crystals leading to the directional growth of the single crystals of calcite that make up the radial design of the coccolith,[10] a property which is hindered in the presence of certain ions or under basic conditions.[13] Whether the CAPs from *G. oceanica* have similar properties at neutral pH or its activity is limited to promoting crystal nucleation remains to be

investigated. While the polysaccharides may indeed modulate calcite morphology during coccolithogenesis, their activity may be modulated inside the cells through the influx of ions or change in pH in the coccolith vesicle, as proposed.[25] Furthermore, it is likely that the cells use other mechanisms to provide morphological control, for instance by controlling the shape of the coccolith vesicle through the cytoskeleton.[26]

It is also important to note that the uronic acid content does not reflect nucleating ability alone, as this was consistent between the two polysaccharides investigated. Additionally, polygalacturonic acid (≥85% uronic acid) alone also showed no effect. As previously proposed,[14] it is very likely that the polysaccharides have their own conformation structures that are important for their activity. Furthermore, it is also possible that other functional groups aside from uronic acids may be involved in the mineralisation process. Since the structure and composition of the CAPs from *G. oceanica* are unknown, further work must be dedicated to identifying the presence of additional functional groups and characterising their roles in promoting crystal nucleation.

It could be argued that the CAPs from *G. oceanica* promote calcite formation by complexing calcium ions and decreasing the supersaturation, hence chancing the kinetics of the crystallisation in favour of the thermodynamic product. However, given the low concentration of CAPs used here compared to the amount of calcium ions in solution (5 µg/ml of CAPs in 5 mM $CaCl_2$ in vaterite-promoting conditions), such effect is highly unlikely. Even polyelectrolytes like polyaspartic acid and polyacrylic acid at concentrations of 10 mg/mL do not significantly lower the concentration of free calcium in the solution.[27] We propose that the polysaccharide either has its own conformational structure, or self-assembles into a structure that is arranged to attract calcium and carbonate ions in a geometry similar to the calcite lattice, therefore acting as a nucleator. As a similar effect is seen even when ethanol is present, it can be assumed that any structure formed by *G. oceanica* is not

disrupted by the change in the solvent system. This is in contrast to the inhibitory properties of *E. huxleyi* CAPs which have been shown to be reduced in the presence of just 1% ethanol.[14] It is also possible another functional group moiety aside from uronic acid may be involved in the mineralization process.

The different properties of *E. huxleyi* and *G. oceanica* CAPs suggests that in each species the polysaccharides play different roles during *in vivo* coccolith biomineralization. Such a stark contrast was unexpected considering that genetic delineation has shown a strong similarity between the two.[15] Further work is required to determine if this property is present in other members of the *Gephyrocapsa* genus and other species, or whether this is unique to *G. oceanica*. Importantly, while questions still remain regarding the solution chemistry of the coccolith vesicle and the precise roles played by the polysaccharides and the baseplate in controlling crystal growth, our results suggest that controls over the vesicle chemistry, and the interactions of the polysaccharide with the mineral phase may be different between *E. huxleyi* and *G. oceanica*. *E. huxleyi* cells are generally considered to exert a strong control over the microenvironment of the coccolith vesicle and to promote calcite by controlling the physical-chemical conditions such as pH and ion concentration.[5c, 28] We also know that *E. huxleyi* is the only coccolithophore known capable of living and reproducing as a naked cell. The fact that *G. oceanica* has a polysaccharide with polymorph-directing properties suggests that in this species the conditions inside the coccolith vesicle may not naturally favour calcite formation, explaining the need for a polymorph-directing agent. As *G. oceanica* has a larger cell size, it is possible that active polymorph selection by a polysaccharide is more energy efficient than promoting calcite by adjustment of the internal vesicle conditions as in *E. huxleyi*.

Another consideration is the role the macromolecules play in coccolithogenesis. The baseplate has been suggested as the nucleation site for calcite in the coccolith

biomineralization process in *E. huxleyi*. However, previous studies on *P. carterae* showed that the polysaccharides work cooperatively with the baseplate to direct Ca^{2+} ions to the mineralization site and promote nucleation.[9, 29] It is possible that *G. oceanica* CAPs are involved in a similar mechanism, and are responsible for nucleation of $CaCO_3$, either alone or co-operatively. As neither the nature or structure of the baseplate in *G. oceanica* has not yet been resolved, more work is needed to elucidate this further.

4. Conclusions

Overall, our results reveal the calcite nucleating ability of *Gephyrocapsa oceanica* coccolith-associated polysaccharide *in vitro*. The polysaccharide is able to actively nucleate calcite under conditions that would promote another polymorph. This property is not found in its closest relation, *Emiliania huxleyi*, suggesting the detailed biomineralization process differs between the two species. It also raises questions as to whether the vesicle solution chemistry and its relationship with seawater chemistry may be different in each of these sister species. We suggest a role as a distinct polymorph selector for the CAPs in the *in vivo* biomineralization process, at least in *G. oceanica*, which has implications for how the biomineralisation process evolved during the taxonomic separation of the two species.

5. Experimental Section

*Materials and general synthesis***:** For direct addition, stock solutions of $CaCl_2.2H_2O$ and Na_2CO_3 in H_2O (HPLC grade) were prepared, and added together to form a final reaction concentration of 0.005 M of each in a 24 well plate with a glass slide at the base. Glass slides were cleaned prior to use with Piranha solution and washed with HPLC grade water and ethanol before drying with compressed air.

For aragonite promoting conditions, stock solutions of $CaCl_2.2H_2O$ and Na_2CO_3 in H_2O (HPLC grade) were prepared. First, Na_2CO_3 was added to the ethanol in a 24 well plate

and mixed, before $CaCl_2.2H_2O$ was also added and mixed to form a total reaction volume of 0.5 mL, and a final reaction concentration of 0.025 M of each. An initial white precipitate formed, and the well plate was placed on a rocker for the requisite length of time at 57 oscillations per minute (opm) to replicate the described 'gentle shaking'.[17]

Extraction of polysaccharides: Polysaccharides were extracted from independent batches of *E. huxleyi* (RCC1216) and *G. oceanica* (RCC1314) cultures at the Department of Earth Sciences, University of Oxford, as previously described.[11a] Briefly, cultures were centrifuged and cleaned using 4.5 % v/v NaOCl and 1 % v/v Triton X-100 in 0.05 % $NaHCO_3$ for 30 minutes at room temperature to remove cellular matter and any extracellular polysaccharides. The samples were subsequently rinsed with MilliQ to remove any residual NaOCl and Triton-X100. The cleaned coccolith mineral was then dissolved using EDTA to release the intracrystalline fraction. This was dialysed to using a 10,000 Da MWCO membrane to remove any small molecules. The intracrystalline fraction was examined by SDS-PAGE and shown to be of one molecular weight (Supporting Information S1), and confirmed not to contain proteins by SDS-PAGE (Supporting Information S2) and Bradford assay. Cultures were grown in K/2 seawater under at 12/12hr dark/light cycle. A stock solution of polygalacturonic acid was prepared in HPLC grade H_2O. Alternatively, the polysaccharides were purified using the method described by de Jong *et al*.[19] and Gal *et al*.[9]

Electron microscopy sample preparation: For cryoTEM, aliquots (3 µL) of reaction solution were applied to a cryoTEM grid and plunge-frozen using a vitrification robot (FEI Vitrobot Mark IV) with the sample application chamber at 21 °C and 100 % humidity. Prior to freezing, cryoTEM grids (Au/C, Quantifoil Micro Tools GmbH) with 2 µm holes were plasma treated using a Quorumtech Glow Discharge system for 45 s. For conventional TEM, the reaction solution was filtered after 24 hours using a 0.22 µm membrane (Millipore) and washed with ethanol. The filtrate was resuspended in ethanol before 3 µL was applied to a

200 mesh C/Ni grid and left to dry. A FEI F20 Technai electron microscope with 200 keV field emission gun, equipped with a Gatan cryoholder operating at ca. -170 °C was used for imaging and LDSAED. Images were recorded on an 8k x 8k CMOS TVIPS F816 camera. For time resolved SEM, aliquots (10 µL) of reaction solution were removed at various time points up to 60 minutes, filtered under vacuum through a 0.22 µm filter membrane (Millipore) and washed with ethanol. Samples were sputter-coated with gold before being imaged using a Zeiss Sigma HD VP Field emission scanning electron microscope. Glass slides were removed from solution and washed with ethanol then sputter-coated with carbon before imaging.

Characterisation: SXPD measurements were taken on the I11 Beamline of the Diamond Light Source, UK,[21] using a wavelength of 0.826054. Strain was analysed using the pseudo-Voigt function, and lattice parameters were calculated using the Scherrer equation. The percentage of aragonite to calcite was determined by Rietveld refinement (R_{exp} <10). Samples were prepared by filtering the entire reaction solution after the requisite amount of time through a 0.22 µm membrane, and the resultant solid transferred to a borosilicate capillary. Coccoliths were extracted from cultures of *G. oceanica* by centrifugation, and were cleaned with NaOCl and Triton X-100 before being transferred to a capillary. Cultures were provided by the Roscoff Culture Collection, France. Powder X-ray diffraction measurements were made using a Bruker D8-Advance diffractometer using a $CuK\alpha_1$ source. Patterns were refined using Topas software. Crystals precipitated from solution on to a glass slide were used to obtain Raman spectra, measured using a Renishaw InVia Raman microscope with a wavelength of 785 nm.

Supporting Information

Supporting Information is available from the Wiley Online Library or from the author.

Acknowledgements

We thank Diamond Light Source for access to beamline I11 (EE14690) that contributed to the diffraction results presented here. This work was supported by the University of Edinburgh and BBSRC, grant no. BB/M029611/1 to FN and ERC Starting Grant (SP2-GA-2008-200915) to RR. The University of Edinburgh EM facility is funded by the Wellcome Trust equipment grant WT087658 and SULSA.

Received: ((will be filled in by the editorial staff))
Revised: ((will be filled in by the editorial staff))
Published online: ((will be filled in by the editorial staff))

References

[1] a) H. A. Lowenstam, S. Weiner, *On Biomineralization*, Oxford University Press, USA **1989**; b) S. Weiner, L. Addadi, *Annu. Rev. Mater. Res.* **2011**, *41*, 21.
[2] F. Meldrum, H. Colfen, *Chem. Rev.* **2008**, *108*, 4332.
[3] J. R. Young, J. M. Didymus, P. R. Bown, B. Prins, S. Mann, *Nature* **1992**, *356*, 516.
[4] J. Young, M. Geisen, L. Cros, A. Kleijne, C. Sprengel, I. Probert, J. Ostergaard, *J. Nanoplankton Res.* **2003**.
[5] a) K. Kayano, K. Saruwatari, T. Kogure, Y. Shiraiwa, *Mar. Biotechnol.* **2011**, *13*, 83; b) M. E. Marsh, *Comp. Biochem. Physiol. B* **2003**, *136*, 743; c) S. Sviben, A. Gal, M. A. Hood, L. Bertinetti, Y. Politi, M. Bennet, P. Krishnamoorthy, A. Schertel, R. Wirth, A. Sorrentino, E. Pereiro, D. Faivre, A. Scheffel, *Nature Commun.* **2016**, *7*, 11228.
[6] a) M. E. Marsh, *J. Struct. Bio.* **2002**, *139*, 39; b) P. v. d. Wal, E. W. d. Jong, P. Westbroek, *Protoplasma* **1983**, *118*, 157.
[7] I. Manton, G. F. Leedale, *J. Mar. Biol. Ass. UK* **1969**, *49*, 1.
[8] a) M. E. Marsh, *Protoplasma* **1994**, *177*, 108; b) A. R. Taylor, C. Brownlee, G. Wheeler, *Annu Rev Mar Sci* **2017**, *9*, 283.
[9] A. Gal, R. Wirth, J. Kopka, P. Fratzl, D. Faivre, A. Scheffel, *Science* **2016**, *353*, 590.
[10] K. Henriksen, S. L. S. Stipp, J. R. Young, M. E. Marsh, *Am. Miner.* **2004**, *89*, 1709.
[11] a) R. B. Y. Lee, D. A. I. Mavridou, G. Papadakos, H. L. O. McClelland, R. E. M. Rickaby, *Nature Commun.* **2016**, *7*, 13144; b) A. M. J. Fichtinger-Schepman, J. P. Kamerling, C. Versluis, J. F. G. Vliegenthart, *Carbohydr. Res.* **1981**, *93*, 105.
[12] N. Ozaki, M. Okazaki, T. Kogure, S. Sakuda, H. Nagasawa, *Thalassas* **2004**, *20*, 60.
[13] K. Henriksen, S. L. S. Stipp, *Cryst. Growth Des.* **2009**, *9*, 2088.
[14] A. Borman, E. W. d. Jong, M. Huizinga, D. J. Kok, P. Westbroek, L. Bosch, *Eur. J. Biochem.* **1982**, *129*, 179.
[15] E. M. Bendif, I. Probert, M. Carmichael, S. Romac, K. Hagino, C. d. Vargas, *J. Phycol.* **2014**, *50*, 140.
[16] a) M. A. Hood, H. Leemreize, A. Scheffel, D. Faivre, *J. Struct. Bio.* **2016**, *196*, 147; b) S. Frolich, H. O. Sorensen, S. S. Hakim, F. Marin, S. L. S. Stipp, H. Birkedal, *Cryst. Growth Des.* **2015**, *15*, 2761.
[17] K. K. Sand, J. D. Rodriguez, E. Makovicky, L. G. Benning, S. L. S. Stipp, *Cryst. Growth Des.* **2012**, *12*, 842.
[18] J. M. Walker, B. Marzec, F. Nudelman, *Angew. Chem. Int. Ed.* **2017**, *56*, 11740.
[19] E. W. de Jong, L. Bosch, P. Westbroek, *Eur J. Biochem.* **1976,** *70*, 611
[20] a) S. Borukhin, L. Bloch, T. Radlauer, A. H. Hill, A. N. Fitch, B. Pokroy, *Adv. Funct. Mater.* **2012**, *22*, 4216; b) D. C. Green, J. Ihli, Y.-Y. Kim, S. Y. Chong, P. A. Lee, C. J. Empson, F. C. Meldrum, *Cryst. Growth Des.* **2016**, *16*, 5174.

[21] S. P. Thompson, J. E. Parker, J. Potter, T. P. Hill, A. Birt, T. M. Cobb, F. Yuan, C. C. Tang, *Rev. Sci. Inst.* **2009**, *80*, 075107.
[22] M. H. Nielsen, S. Aloni, J. J. d. Yoreo, *Science* **2014**, *345*, 1158.
[23] J. W. Morse, R. S. Arvidson, A. Luttge, *Chem. Rev.* **2007**, *107*, 342.
[24] A. Berman, J. Hanson, L. Leiserowitz, T. F. Koetzle, S. Weiner, L. Addadi, *Science* **1993**, *259*, 776.
[25] a) C. Brownlee, A. Taylor, in *Coccolithophores - From Moleucular Scale Processes to Global Impact* (Eds: H. Thierstein, J. R. Young), Springer Verlag, Berlin/Heidelberg **2004**, p. 31; b) A. R. Taylor, C. Brownlee, G. Wheeler, *Annu. Rev. Mar. Sci.* **2017**, 283.
[26] G. Langer, L. J. d. Nooijer, K. Oetjen, *J. Phycol.* **2010**, 1252.
[27] a) D. Gebauer, H. Colfen, A. Verch, M. Antonetti, *Adv. Mater.* **2009**, *21*, 435; b) A. Verch, D. Gebauer, M. Antonetti, H. Colfen, *Phys. Chem. Chem. Phys.* **2011**, *13*, 16811.
[28] A. Gal, S. Sviben, R. Wirth, A. Schrieber, B. Lasalle-Kaiser, D. Faivre, A. Scheffel, *Adv. Sci.* **2017**, *4*, 1700088.
[29] A. Gal, R. Wirth, Z. Barkay, N. Eliaz, A. Scheffel, D. Faivre, *Chem. Commun.* **2017**, *53*, 7740.

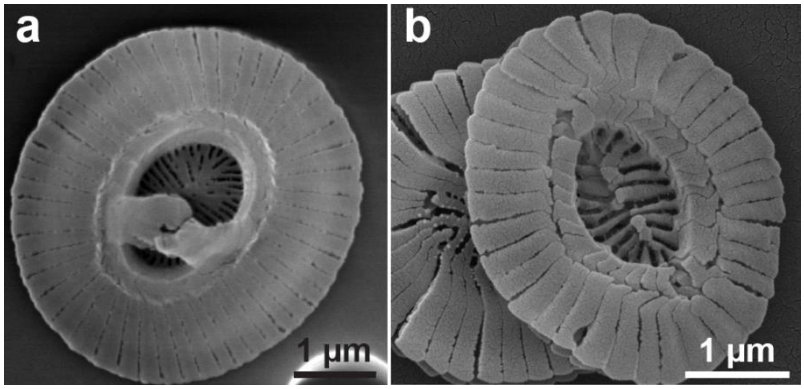

Figure 1. a) *G. oceanica* coccolith and b) *E. huxleyi* coccolith examined by SEM

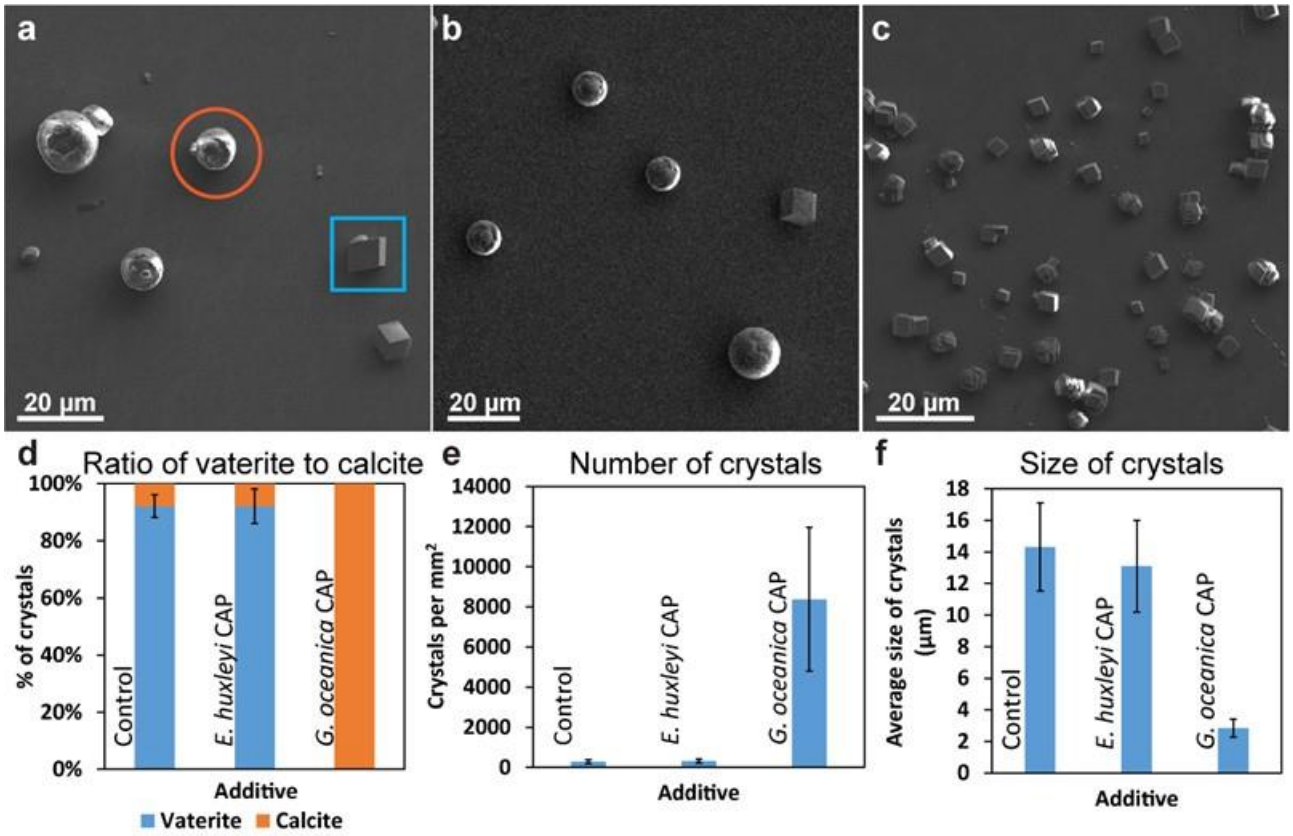

Figure 2. Top: SEM images of glass slides from the base of direct addition reactions after 20 minutes with a) no additives, (spherical vaterite shown with an orange circle, rhombohedral calcite denoted by the blue square) b) *E. huxleyi* CAPs at 5 µg/mL and c) *G. oceanica* CAPs at 5 µg/mL.
Bottom: Statistical data from a minimum of 300 crystals per sample imaged by SEM (each experiment was repeated three times, and although the absolute numbers differed slightly the effect was consistent). d) The ratio of vaterite to calcite for the control with no additives, *E. huxleyi* CAPs and *G. oceanica* CAPs, showing the 100% calcite obtained with *G. oceanica* CAPs. e) The number of crystals per mm2 formed in each reaction. f) Average size of the crystals formed in µm.

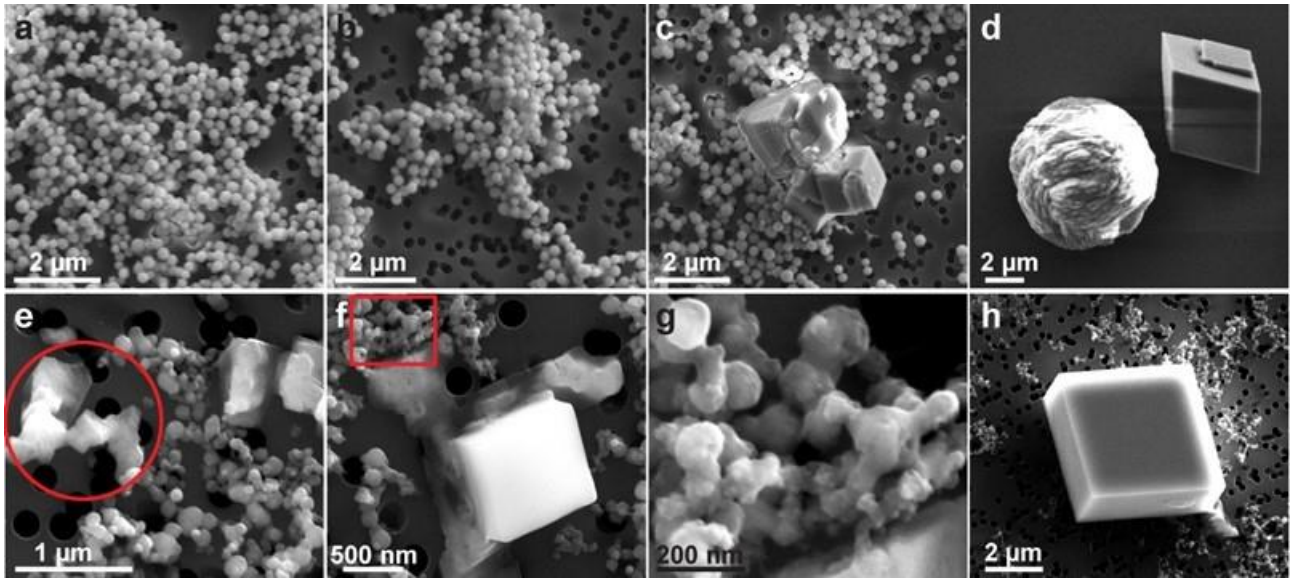

Figure 3. SEM images of the reaction solution with no additives filtered after a) 1 minute. ACC particles of 250-350 nm are visible. b) After 3 minutes the particles have begun to group together, and not until c) 10 minutes is crystalline material present. d) Finally, after 20 minutes, both vaterite (spherical) and calcite (rhombohedral) crystals were present. e) When *G. oceanica* CAPs were present after 1 minute, small ACC (50-150 nm) is present alongside semi cuboid shapes (red circle). f) After 3 minutes, calcite rhombohedrons were already visible, surrounded by flat material and angular ACC particles (magnification of red box shown in g). h) After 10 minutes, rhombohedral calcite was fully formed with a small amount of ACC around.

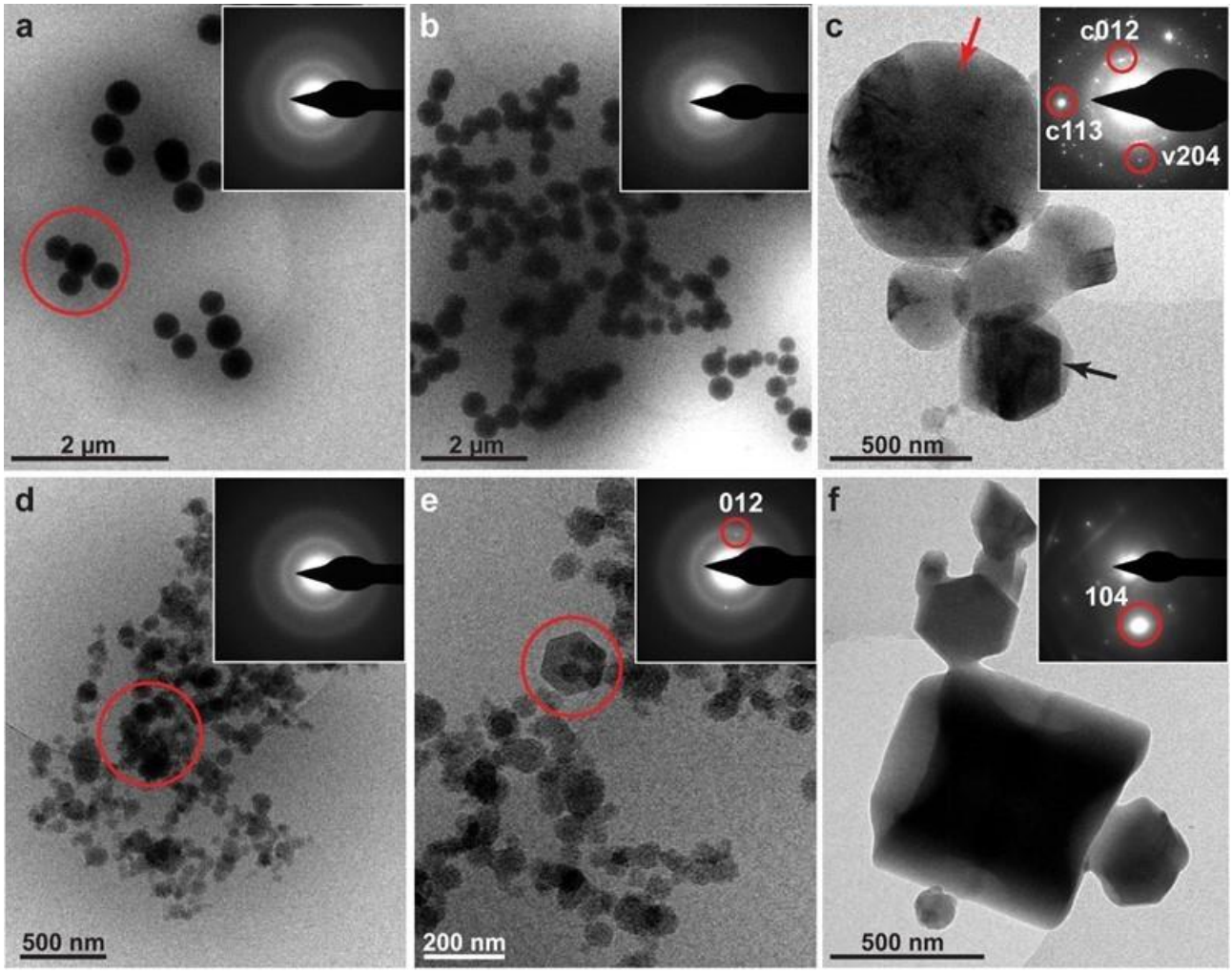

Figure 4. CryoTEM images of the reaction solution after a) 1 minute with no additives showing a small amount of ACC particles of 250-350 nm (red circle), shown to be amorphous by the associated LDSAED, inset. b) After 10 minutes, the amount of ACC has increased and begun to aggregate, but remained amorphous (LDSAED, inset). c) By 20 minutes, crystals of both vaterite (top, red arrow) and calcite (bottom, black arrow) were present, confirmed by attached LDSAED which shows the *(012)*- and (*113*)-planes of calcite and the (*204*)-plane of vaterite. d) When *G. oceanica* CAPs were present in the reaction solution, after 1 minute small, irregular shaped ACC particles (45-100 nm) were visible which are shown to be amorphous by the LDSAED, inset. e) After 3 minutes the amorphous material had begun to crystallise, with small 80 nm calcite crystal visible confirmed by the (*012*)-plane visible in the associated LDSAED pattern (inset). f) The final stage after 40 minutes showed only calcite present, with the (*104*)-plane clear in the LDSAED (attached).

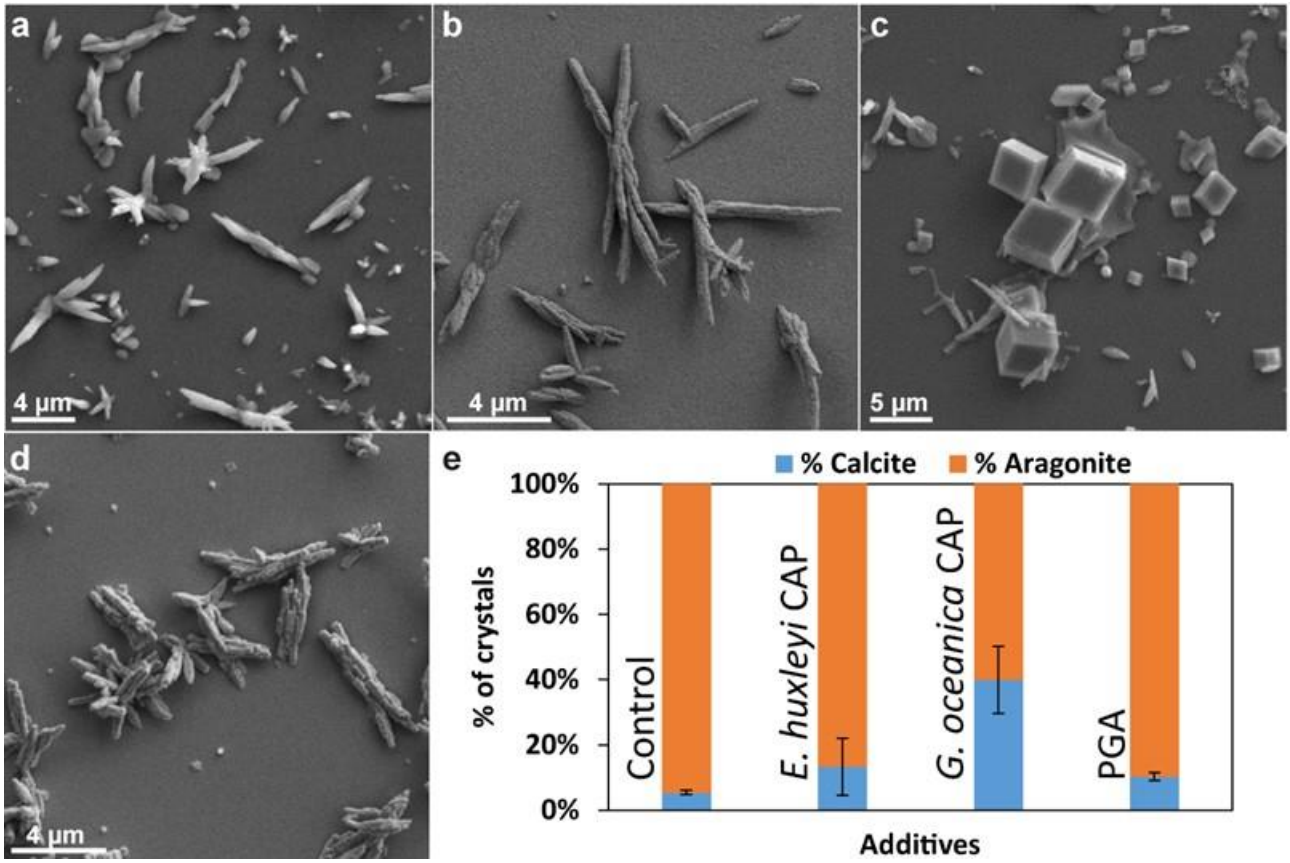

Figure 5. SEM images of glass slides from the base of the aragonite promoting reaction after 24 hours with a) no additives, b) *E. huxleyi* CAPs, c) *G. oceanica* CAPs and d) polygalacturonic acid. e) A graph comparing the % of calcite to aragonite in the system from refined powder X-ray diffraction patterns for each additive.

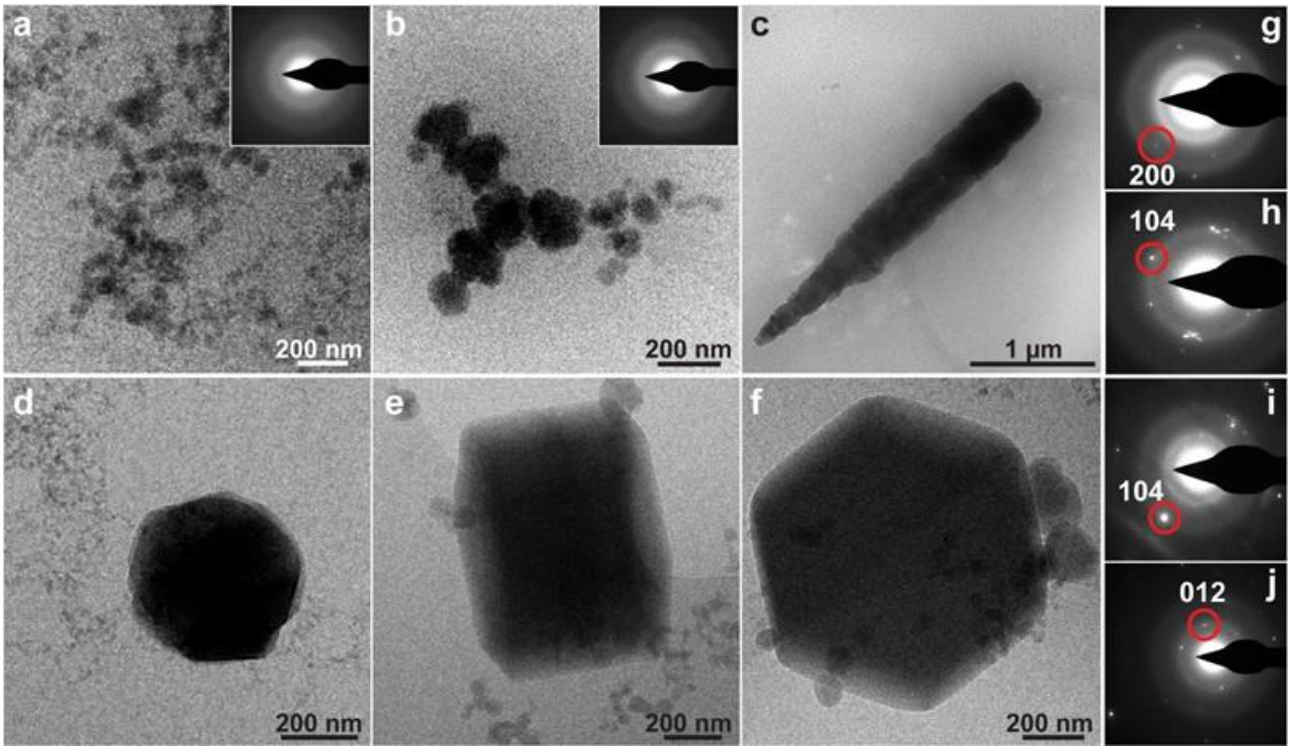

Figure 6. CryoTEM images of reaction solution of the aragonite promoting system with no additive (a-c) and with *G. oceanica* CAPs (d-f). a) Control after 3 minutes showing small ACC particles (LDSAED inset). b) After 10 minutes, the small ACC had agglomerated into larger particles which remain amorphous (LDSAED inset). c) After 1 hour, small crystalline aragonite needles were visible, as shown by the associated LDSAED (g). d) When *G. oceanica* CAPs were present, after 1 minute a calcite crystal was already forming, with crystalline reflections visible in the LDSAED (h). e) After 5 minutes calcite crystals continued to form (LDSAED shown in i)). f) Calcite crystals continued to form after 40 minutes (LDSAED, k). g) LDSAED for c). h) LDSAED for d). i) LDSAED for e) and k) LDSAED for f).

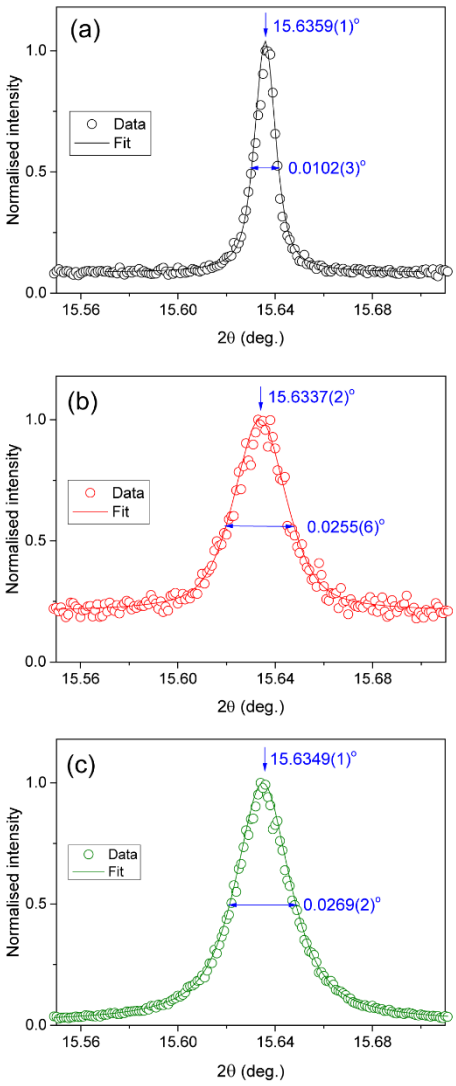

Figure 7. Calcite (*104*)-reflections for the reaction solutions after 24 hours from HR-PXRD, in the direct addition system for crystals grown without additives (a, black) and in the presence of *G. oceanica* CAPs (b, red), and biogenic crystals (c, green). Both the original (circles) and fitted (line) data is presented. Arrows mark the centre of the reflection accompanied by the 2θ value in degrees. Broadening is demonstrated by the double ended arrows and associated values in degrees.

Coccolith-associated polysaccharides from Gephyrocapsa oceanica are shown to have the ability to directly nucleate calcite even when this is no longer the thermodynamically favoured polymorph. This property was not shared by CAPs extracted from its "sister species" Emiliania huxleyi, suggesting that CAPs may have different functions in different species.

Coccolithophores, biomineralization, calcite, cryo-transmission electron microscopy, crystal nucleation

Jessica M. Walker, Bartosz Marzec, Renee B. Y. Lee, Kristyna Vodrazkova, Sarah J. Day, Chiu C. Tang, Rosalind E. M. Rickaby, Fabio Nudelman*

Polymorph Selectivity of Coccolith-Associated Polysaccharides from *Gephyrocapsa oceanica* on Calcium Carbonate Formation *In Vitro*